Int. J. Heat Mass Transfer. Vol. 29, No. 9, pp. 1319–1332, 1986
Printed in Great Britain

0017–9310/86 $3.00 + 0.00
Pergamon Journals Ltd.

Vapor condensation onto a turbulent liquid—I. The steady condensation rate as a function of liquid-side turbulence†

AIN A. SONIN, MARTIN A. SHIMKO‡ and JUNG-HOON CHUN§
Department of Mechanical Engineering, Massachusetts Institute of Technology, Cambridge, MA 02139, U.S.A.

(*Received* 20 *June* 1985 *and in final form* 30 *December* 1985)

Abstract—Data are presented for the rate of vapor condensation onto a turbulent liquid, the turbulence being isotropic in the horizontal plane and bulk-flow free, and the interface being shear-free and relatively free of waves. A correlation is proposed for the rate coefficient in terms of the liquid-side turbulence intensity, turbulence macroscale and subcooling.

1. INTRODUCTION

IN MANY situations which involve heat or mass transfer across a gas–liquid interface, the liquid is in turbulent motion and the transport rate is controlled by conditions on the liquid side. One example is gas absorption into liquids, with applications in environmental problems as well as in chemical processing. Another is direct-contact condensation of vapor on flowing liquid, a problem which is of considerable interest as a driving force in nuclear reactor transients and accident scenarios as well as in two-phase flows in general.

A survey of the literature shows that although various correlations have been proposed for the interfacial transport rate, based usually on a combination of experimental information and simplistic conceptual models, there is disagreement between the proposed correlations, and a unified view of the liquid-side transport mechanism is lacking. Transport into a liquid surface is intimately tied to the turbulence structure very near the interface. Our present understanding of that structure is largely speculative, and no consensus exists on a basic theoretical model which might serve as the starting point for describing all turbulent, free-surface transport problems.

The present paper gives experimental results for the transport coefficient for what is perhaps the simplest case: a shear-free and relatively wave-free horizontal interface with a liquid-side turbulence which is isotropic in the horizontal plane and free of bulk flow (except, of course, for the vertical bulk flow caused by the condensation itself). The experiments are for atmospheric steam condensing on subcooled water. The dependence of the condensation coefficient on turbulence intensity, turbulence macroscale and bulk water temperature is examined, a correlation is proposed, and some conclusions on the nature of the transport mechanism are offered. The hope is that the correlation will not only be useful in itself, but will eventually serve as a convenient testing ground for fundamental theoretical models.

A companion paper [1] shows that condensation on a free surface becomes unstable at sufficiently high liquid-side turbulence intensities. The instability gives rise to intermittent, burst-like condensation events with very high intensity but short duration.

2. CONCEPTUAL MODELS FOR LIQUID-SIDE TRANSPORT COEFFICIENT AT SURFACE

2.1. *Heat and mass transport with negligible normal bulk flow*

The liquid-side transport resistance is usually expressed in terms of a transport coefficient k which has the units of velocity. For mass transfer the coefficient is defined as

$$k = \frac{j}{\Delta c} \tag{1}$$

where j is the molar flux and Δc is the molar concentration difference between the surface and the bulk of the liquid. For heat transport one can define an equivalent quantity

$$k = \frac{q}{\rho c_p \Delta T} \tag{2}$$

where q is the heat flux, ρ is the liquid's density, c_p is the liquid's specific heat, and ΔT is the temperature difference between the surface and the bulk of the liquid. Conceptual models for heat transport are similar to those for mass transport, the only difference, apart from the definition of k, being that where the mass diffusivity D and the Schmidt number Sc appear in one, the thermal diffusivity α and the Prandtl number Pr appear in the other.

† Work supported by the U.S. Nuclear Regulatory Commission under Grant NRC-G-04-83-004.
‡ Presently at Thermo Electron Corporation.
§ Presently at Mixalloy Corporation.

NOMENCLATURE

A interface area, $\pi D^2/4$
c_p specific heat of liquid at constant pressure
C_μ coefficient in K–ε model
Δc molar concentration difference between the surface and bulk of the liquid
d nozzle diameter (Fig. 1)
D system diameter (Fig. 1)
h_{fg} latent heat of condensation
j molar flux across interface
k mass transport coefficient, $j/\Delta c$
k_c condensation coefficient, equation (9)
K turbulence intensity in K–ε model
L length scale in K–ε model, $K^{3/2}/\varepsilon$
$\dot{m}_c$ condensation mass flux across interface
Pr_s Prandtl number based on liquid conditions at surface, $c_{ps}\mu_s/\lambda_s$
q heat flux into liquid at surface
Q water volume flow rate circulating through system (Fig. 1)
Re system Reynolds number, $(Q/Dd)(D/\nu)$
Re_s turbulence Reynolds number based on liquid conditions at the surface, $\rho_s v_s' D/\mu_s$
t time
T local liquid temperature
T_{in} temperature of water injected into test system (Fig. 1)
T_w bulk liquid temperature
ΔT liquid subcooling, $T_s - T_w$
u^* shear velocity based on interfacial stress and liquid density
u' r.m.s. value of streamwise velocity fluctuations in system with flow
v characteristic turbulence velocity (usually, r.m.s. value)
v' r.m.s. value of the local horizontal or vertical component of turbulent velocity in the system of Fig. 1
v_s' the value of v' extrapolated from the bulk of the liquid to the surface, disregarding surface damping
V volume of water in test cell
y coordinate measured from surface into bulk of liquid
z coordinate measured vertically upward from the nozzle in the system of Fig. 1
z_0 reference value of z.

Greek symbols
α thermal diffusivity of liquid
α_T turbulent thermal diffusivity
β coefficient defined by equation (14)
δ thermal layer thickness, equation (32)
ε viscous dissipation rate in K–ε model
λ thermal conductivity of liquid
Λ integral length scale of turbulent eddies
μ liquid viscosity
ν liquid kinematic viscosity
ρ liquid density
σ surface tension coefficient
σ_K coefficient in K–ε model
τ contact time, see equations (3), (5) etc.
$\phi(Re)$ function defined in Fig. 4.

Subscripts
0 evaluated at reference point $z = z_0$
s evaluated at (liquid) interfacial conditions (see above for v_s' and Re_s, however).

The various conceptual models which have been proposed for the turbulent transport mechanism view the process either in terms of 'surface renewal', where transport occurs by transient molecular diffusion into the turbulent eddies which sweep by the surface periodically, or in terms of a steady, Reynolds-averaged, turbulent diffusion. The two ways of viewing the process give essentially identical results if based on the same physical assumptions. The variety in the available models arises [2] because there is no consensus on the actual turbulence structure very near the free liquid interface, where the fluctuations in the vertical velocity component are damped out.

In the surface renewal approach one argues [3] that if a typical eddy spends a time τ in contact with the interface, and transport occurs by molecular diffusion into the eddy during this time, the liquid-side transport coefficient should be

$$k \sim (\alpha/\tau)^{1/2} \tag{3}$$

where α is the molecular diffusivity (in what follows, the models will be discussed in terms of heat transfer, in which case α is the thermal diffusivity). The problem is thus reduced to that of determining how the contact time depends on turbulence characteristics.

The steady, turbulent diffusion approach is based on the Reynolds-averaged temperature (or, in the case of species transport, concentration) equation, with the Reynolds flux term approximated in terms of an effective turbulent diffusivity α_T. Levich [4] and others have argued that the turbulent diffusivity α_T very near a free surface should increase as the square of the distance y below the interface, i.e. that

$$\alpha_T = y^2/\tau \tag{4}$$

where τ is a coefficient with dimensions of time whose magnitude depends on turbulence conditions near the interface. With equation (4) the species concentration equation can be integrated to yield the transport coefficient as [5]

$$k = \frac{2}{\pi}(\alpha/\tau)^{1/2} \tag{5}$$

which is essentially identical to the result previously obtained by the surface renewal approach if the time scales are interpreted to be the same quantity, or at least proportional to each other.

With either approach, the problem thus reduces to that of determining how the time scale τ associated with transport-controlling turbulent eddies at the interface depends on the liquid properties, flow conditions and interfacial characteristics such as surface tension.

Virtually no direct information is available on the structure of the turbulence very near a free surface. Basic theory is nonexistent; some experimental data on eddy diffusivity [6] are available only outside the diffusion sublayer near the surface, that is, outside the region that actually controls the transport rate. This has left the field open to considerable conjecture, the aim being to fit as much of the available transport data as possible with some (invariably simplified) assumptions about what controls the parameter τ.

Table 1 lists six major conceptual models which have been proposed in the literature. Each model is based on particular simplifying assumptions about how τ is controlled by the characteristic turbulence velocity v in the bulk of the liquid (usually taken as the r.m.s. value of the velocity fluctuations, or as the friction velocity if the problem involves an applied shear), the integral length scale Λ of the turbulence (the eddy size), the liquid's kinematic viscosity ν and density ρ, and the interfacial surface tension σ. The list is limited to models which do not depend explicitly on gravity. Surface tension plays a role only in Levich's model.

The large-eddy model [7] assumes that surface transport is controlled by the macroscale of the turbulence in the liquid, while the small-eddy model [8] attributes control to the eddies of the Kolmogorov microscale based on turbulence conditions in the bulk of the liquid. The viscous inner-layer model, which is usually applied to cases where the free surface is under an applied shear, assumes that the turbulence near the interface can be correlated in a dimensionless form similar to the law of the wall, with the friction velocity u^* serving as the characteristic value of v. Alternatively, one can derive the inner-layer model by assuming that the small-eddy concept applies, but that the Kolmogorov microscale should be computed from the velocity v and the local inner-layer length scale ν/v^2 near the surface [9, 10]. Henstock and Hanratty's model [11] falls somewhere between the large-eddy and viscous inner-layer models; their assumption is that equation (4) should have a form such that the turbulent diffusivity reaches the bulk (undamped) value $v\Lambda$ not in the distance Λ from the interface as in the large-eddy model, but in the distance ν/v associated with the viscous inner-layer scaling. Levich's model [4] is similar in spirit to the large-eddy model, except that he assumes that the eddies which sweep the surface are not the same size as in the bulk of the liquid, but have a size controlled by the amount

Table 1. Major conceptual models for transport across surface

Model	Assumptions: Diffusivity α	Assumptions: Time scale τ	Transport coefficient $k = c(\alpha/\tau)^{1/2}$
1. Large-eddy model [7]	α	Λ/v	$k/v = c_1 Pr^{-1/2}(v\Lambda/\nu)^{-1/2}$
2. Small (Kolmogorov) eddy model [8]	α	$(\nu\Lambda/v^3)^{1/2}$	$k/v = c_2 Pr^{-1/2}(v\Lambda/\nu)^{-1/4}$
3. Viscous inner-layer model	α	ν/u^{*2}	$k/u^* = c_3 Pr^{-1/2}$
4. Henstock and Hanratty [11]	α	$\nu^2/v^3\Lambda$	$k/v = c_4 Pr^{-1/2}(v\Lambda/\nu)^{1/2}$
5. Levich [4]	α	$\sigma/\rho v^3$	$k/v = c_5 Z\, Pr^{-1/2}(v\Lambda/\nu)^{1/2}$
6. Kishinevsky [12]	$v\Lambda$	Λ/v	$k/v = c_6$

α = molecular diffusivity; v = characteristic turbulent fluctuating velocity; u^* = shear velocity; Λ = integral length scale of turbulent eddies; ν = kinematic viscosity; ρ = density; σ = surface tension; $Pr \equiv \nu/\alpha$ (Prandtl number); $v\Lambda/\nu$ (eddy Reynolds number); $Z \equiv (\nu^2\rho/\sigma\Lambda)^{1/2}$ (Ohnesorge number), c_1–c_6: constants.

of surface curvature allowed by the surface tension forces. This implies that Λ in the large-eddy model is to be replaced by $\sigma/\rho v^2$. The model of Kishinevsky [12] is intended for very high levels of turbulent agitation, his idea being that transport then takes place by fully turbulent diffusion into the liquid rather than by molecular diffusion into the surface-renewing eddies which are characteristic of the turbulence. This would suggest that the molecular diffusivity α should be replaced by the bulk turbulent diffusivity $v\Lambda$ and that $\tau \sim \Lambda/v$.

Each of these models claims at least some support from experimental data. Fortescue and Pearson [7] compared their large-eddy model favorably with data from a shallow channel flow where turbulence was induced by a grid. Theofanous *et al.* [13] argued that the bulk of the data then available, which included open-channel flows, supported the small-eddy model at eddy Reynolds numbers $v\Lambda/\nu$ greater than about 500, and the large-eddy model at Reynolds numbers smaller than 500. It should be noted, however, that the turbulence conditions were not measured directly in the experiments on which these comparisons were based, and the investigators had to make some interpretations and deal with significant data scatter.

The more recent data on transport of both mass and heat into open-channel flows (see refs. [9, 10, 14, 15] for flows driven by shear at the surface and refs. [16, 17] for gravitation-driven flows with no shear at the surface) support the viscous inner-layer model, at least at eddy Reynolds numbers which are not too small, and contradict the suggestion of Theofanous *et al.* [13] that the large-eddy model should apply at lower eddy Reynolds numbers [15]. The coefficient c_3 in Table 1 is not universal, however, and appears to depend on how the turbulence is generated. If the velocity v in the model equation is taken (as it usually is in the literature) as the shear velocity u^*, c_3 has one value for the data where the shear is applied at the surface and another for the gravitational flow data, where u^* is based on the shear at the bottom and the surface is shear free. An interpretation of v as the flow-wise r.m.s. velocity at the surface, using the correlations in refs. [18, 9] between that velocity and u^*, brings the two values of the coefficient closer, but not into coincidence (see Section 5).

Curiously, although the inner-layer model appears to describe the surface transport in moderately inclined, open-channel flows, it does not properly describe thin, vertically falling films. For those, the body of the available data appears to support something closer to the model of Henstock and Hanratty [11] although recent reviews [19, 20] suggest that surface waves in falling films bring in a dependence on both surface tension and gravity waves, and that the problem is more complicated than the Henstock–Hanratty model admits.

The Kishinevsky model also claims some experimental support [21], albeit only at very high levels of turbulent agitation. Presumably, this model applies when the turbulence is so intense that surface breakup occurs and the transport into the liquid is controlled by volumetric entrapment of gas bubbles into the liquid rather than by molecular diffusion into the surface-renewing turbulent eddies.

Finally, it should be pointed out that while the $\alpha^{1/2}$ dependence, which is implied by all models in Table 1 except Kishinevsky's, has become accepted in much of the literature and has some support from careful experiments (e.g. [22]), at least at high Schmidt or Prandtl numbers, dependences ranging from $\alpha^{1/2}$ to α^1 have been reported in some experimental studies (e.g. [23]).

In summary, the literature contains a number of different conceptual models for the free surface transport coefficient in terms of liquid-side turbulence parameters, even for the simplest case where waves are not a controlling factor and the interface is clean. The dependence of k on r.m.s. velocity in Table 1 ranges from a power of 1/2 to a power of 3/2, and the dependence on integral length scale from a power of $-1/2$ to a power of 1/2. What is more, although some serviceable correlations have been obtained for specific flow configurations, notably channel and falling film flows, there is at present no unified view of the surface transport mechanism, and no consensus about how the turbulence in the liquid controls the surface transport rate.

2.2. *Condensation*

Condensation is controlled on the liquid side by the rate at which the latent heat is transported from the surface to the bulk. On the liquid side, therefore, condensation appears essentially as a heat transport process, but one which differs from heat transport without phase change in that it is accompanied by the condensation-induced bulk convection normal to the interface. The latter brings about a change in the conceptual models reviewed above. The point can be illustrated in terms of the steady, turbulent diffusivity model [5] to which is added a convective term. In the one-dimensional case the Reynolds-averaged temperature in the liquid is governed by

$$(\dot{m}_c/\rho)\frac{dT}{dy} = \frac{d}{dy}\left[(\alpha + y^2/\tau)\frac{dT}{dy}\right] \tag{6}$$

where y is the distance measured from the interface into the liquid, $\dot{m}_c/\rho$ is the bulk liquid flow speed in the y-direction due to the condensation, $\dot{m}_c$ being the mass flux density due to condensation at the surface and ρ the liquid density, α is the molecular thermal diffusivity, and equation (4) has been used for the turbulent thermal diffusivity. Equation (6) can be integrated from $y = 0$, where the liquid is at its saturation temperature T_s, and the heat flux is

$$-\rho c_p \alpha (dT/dy)_{y=0} = \dot{m}_c h_{fg} \tag{7}$$

h_{fg} being the latent heat of condensation, to $y \to \infty$,

where the liquid is at the bulk temperature T_w. This yields

$$k_c = \frac{2}{\pi}(\alpha/\tau)^{1/2}(h_{fg}/c_p\Delta T)\ln(1+c_p\Delta T/h_{fg}) \quad (8)$$

where $\Delta T = T_s - T_w$ is the liquid's subcooling, and

$$k_c \equiv \dot{m}_c h_{fg}/\rho c_p \Delta T \quad (9)$$

is a 'condensation coefficient' analogous to the transport coefficient of equation (2) with the heat flux taken from equation (7).

For $c_p\Delta T/h_{fg} \ll 1$, as is the case with steam condensing on water, equation (8) can be expanded to first order as

$$k_c = \frac{2}{\pi}(\alpha/\tau)^{1/2}(1-c_p\Delta T/2h_{fg}). \quad (10)$$

Comparing with equation (5), we see that at the same turbulence conditions (τ) and diffusivity (α), the condensation coefficient is somewhat smaller than the ordinary heat transport coefficient. This difference arises because the bulk flow due to condensation distorts the temperature profile and reduces the temperature gradient on the liquid side of the interface. For atmospheric steam condensing on 30°C water, $c_p\Delta T/h_{fg} = 0.13$ and, insofar as equation (6) is applicable, k_c is smaller than the ordinary coefficient k by 7%.

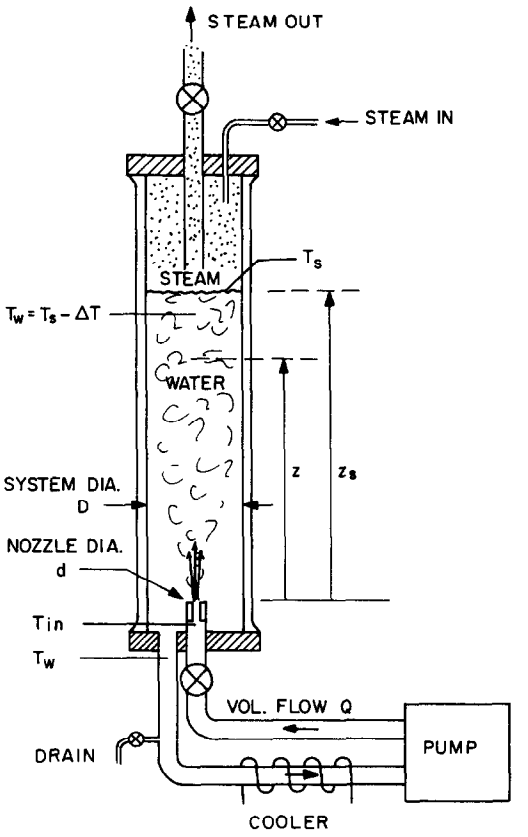

FIG. 1. Test cell.

3. EXPERIMENTAL APPARATUS AND METHODS

Test cell

The apparatus is shown in Fig. 1. The test cell is a vertical Pyrex tube of diameter D, partially filled with water. A steady turbulence is created in the water by an axial jet which is directed toward the surface from below, with the water circulating in a closed loop through a pump and a cooler. The key to the design is the placement of the nozzle deep in the tube, more than $3D$ below the water level. Experiments suggest [24] that at an elevation of about $z \sim 3D$ (see Fig. 1), the jet fills the tube cross-section, the characteristic eddy size becomes locked to the diameter and the turbulent velocity fluctuations begin to dominate over the mean circulatory velocity. At higher elevations, the system is characterized by an approximately bulk-flow-free turbulence with a constant integral length scale proportional to tube diameter and an intensity which is approximately uniform and isotropic in a horizontal plane, although it decays with distance z from the nozzle.

Two geometrically similar test cells were used, their sizes differing by a factor of four (Table 2).

The jet system has some advantages over systems which produce the turbulence by oscillating a grid below the surface (e.g. [25–27]). First, it is a purely hydraulic, steady flow system in which the turbulence intensity can be easily controlled via the jet momentum flux (more on this later). Second, the imprint left by a small nozzle on the turbulence structure appears to disappear at much shorter distances z than that left by a typical oscillating grid.

Steam and water

Condensation heat transfer was imposed at the surface by circulating pure steam at slightly above atmospheric pressure in the region above the water. The steam came from the Massachusetts Institute of Technology steam supply which typically has an air mass fraction of the order of 10^{-4}. The steam was passed through a steam–water separator and a 75 dm³ holding tank which served as an air separator, the steam being removed from the top of the tank and any air being allowed to settle toward the bottom from which it was purged. This provided a slightly superheated steam which was relatively free of air. To further

Table 2. Test cell dimensions

		System	
		Large	Small
Cell diameter	D (cm)	15.3	3.8
Nozzle diameter	d (cm)	0.64	0.16
Ratio	D/d	24	24

guard against the accumulation of noncondensable gases at the water surface, an excess amount of steam was passed through the cell, and the exhaust pipe was designed so as to provide a scouring of the surface with the excess steam without changing the turbulence imposed from below the surface. This was done experimentally by ensuring that the condensation rates were independent of both the distance of the exhaust pipe from the surface and the steam flow rate. In addition, steam temperature was monitored with a thermocouple near the surface; a decrease in that temperature below saturation would indicate buildup of noncondensables.

The experiments were done with tap water. A small amount of water was continuously drained from the test section to maintain constant water volume and level.

Bulk water temperature was measured with a movable thermocouple (accuracy 0.5 K). Turbulent mixing in the bulk of the liquid was effective: the water temperature was essentially constant to within millimeters of the free surface. Based on the heat transfer data, the thermal diffusion layer thickness at the surface was estimated as being of the order of 0.1 mm (see Section 5).

Condensation rate measurement

Condensation rates were determined from the steady-state rise in water temperature between the inlet and outlet of the test cell. An application of the first law to the (insulated) test cell yields

$$k_c = \frac{Q(T_w - T_{in})}{A\Delta T} \frac{1}{(1 + c_p \Delta T / h_{fg})} \tag{11}$$

where k_c is the condensation coefficient defined in equation (9), Q is the water volume flow rate through the pump, $T_w - T_{in}$ is the temperature rise from the nozzle exit plane to the water exhaust (the latter being essentially at the bulk temperature T_w), and $A = \pi D^2/4$ is the surface area.

The experimental values of k_c were determined from equation (11) using measured values of Q, ΔT and $T_w - T_{in}$. The measurements had two critical components. One was the determination of $T_w - T_{in}$, which was in the range 1.4–9 K, a typical value being 5 K. This was done with two thermistor gages (Omega ON-970-44007) in a Wheatstone bridge arrangement, with an estimated accuracy of ± 0.2 K, i.e. 4% of the typical measurement. The other was to ensure that a steady state had indeed been attained, that is, that the temporal rate of energy increase of the water in the test cell was small compared with the condensation heat flux. The criterion for this can be shown to be

$$\frac{dT_w}{dt} \ll (T_w - T_{in}) \frac{Q}{V} \tag{12}$$

where V is the volume of water in the test cell. T_w was monitored on a recorder to ensure that sufficient time had elapsed for equation (12) to be satisfied.

Two further comments are in order. First, the use of the tube cross-sectional area A for the surface implies small area increase due to surface waviness. Only data with small surface waviness (less than about 1 cm peak-to-peak in the 15.2 cm diameter system) are reported in this paper; this put an upper bound on the usable turbulence intensities. Secondly, since our present objective was to investigate the effect of turbulence without the complication of thermal stratification, care had to be taken to avoid damping of the jet-imposed turbulence by stable thermal stratification near the surface. Thermal stratification, when present, made itself visible as a thin, shimmering layer at the surface, and brought about a reduction in the condensation coefficient. It was found experimentally that stratification could be avoided by keeping the r.m.s. value of the turbulent velocity fluctuations (defined as v_s' later) well above 0.02 m s^{-1}. This put a lower bound on the usable turbulence intensities.

Velocity measurements

Fluctuating and mean velocities were determined by seeding the water with 3 mm diameter polypropylene spheres (specific gravity 0.91), taking video film at 120 frames s^{-1}, and recording samples of particle displacement between successive frames, in each case choosing particles which were closest to the nominal elevation z. The horizontal sampling region extended essentially from the axis to a radius 2/3 that of the cell. Each velocity data point is based on at least 60 samples taken at 100-frame intervals.

The polypropylene spheres follow the turbulent fluid accelerations closely because their density is close to that of water. Assuming a low Reynolds number Stokes drag law, the maximum expected difference between particle and fluid velocities was estimated to be about 7% [28]. In fact, the particle Reynolds number based on relative velocity was not small compared with unity, which means that the actual particle drag exceeded the Stokes formula, and hence the 7% should be an overestimation of the velocity difference.

4. STEADY-STATE DATA CORRELATIONS

4.1. *Turbulence calibration*

An approximate analytical model for high Re. An idea of the turbulence distribution in the cell can be obtained by applying the K–ε model of turbulence to the region $z/D > 3$ where the mean circulatory flow is small compared with the fluctuating velocities and the turbulence intensity K can be approximated as a function of z alone. The high Reynolds number form of the K–ε model [29] simplifies to

$$0 = \frac{d}{dz}\left[\frac{C_\mu}{\sigma_K} K^{1/2} L \frac{dK}{dz}\right] - \frac{K^{3/2}}{L} \tag{13}$$

where $C_\mu = 0.09$ and $\sigma_K = 1.0$ [30]. The length scale $L = K^{3/2}/\varepsilon$ in the model (ε being the dissipation function) is assumed to be locked to the tube diameter,

that is

$$L = \beta D \tag{14}$$

where β is a constant. The effect of the tube boundaries enters through this constraint, even though the equation for K is written in a one-dimensional approximation.

Experiments showed (see below) that the precise location $z = z_s$ of the free surface had a negligible effect on the turbulence sufficiently far below the damped layer. Hence, provided z is not too close to the free surface, equations (13) and (14) can be solved with the boundary condition $K \to 0$ at $z \to \infty$. The result is

$$K^{1/2} = K_0^{1/2} \exp\{-\beta^{-1}(\sigma_K/6C_\mu)^{1/2}(z/D - z_0/D)\} \tag{15}$$

where K_0 is the magnitude of K at $z = z_0$. The reference location must be at $z/D > 3$, consistent with our approximations.

$K^{1/2}$ is proportional to the r.m.s. velocity component v'. At high Reynolds numbers the reference value v_0 should depend only on the fluid density ρ, the system size D, and the jet momentum flow rate $4\rho Q^2/\pi d^2$, the assumption being that z is in the jet's far field. Dimensional analysis therefore suggests that

$$K_0^{1/2} = \text{const.}\, Q/Dd \tag{16}$$

and hence, it follows from equation (15) that

$$v' = b(Q/Dd)\exp(-1.36z/\beta D) \tag{17}$$

where b is a constant, and we have used Pope and Whitelaw's [30] values of σ_K and C_μ.

Insofar as equation (17) is applicable, it implies that a calibration of the system [i.e. a determination of the coefficients b and β in equation (17)] can be achieved by a minimum of two controlled measurements of v' at different z.

Experimental calibration. In the general case where the high Reynolds number limit implied by the K–ε model may not necessarily have been attained, v' will depend on D, z, ρ, the liquid's kinematic viscosity ν, and the jet momentum flow rate $4\rho Q^2/\pi d^2$; the assumptions again being that z is in the jet's far field (i.e. at sufficiently large z/D) and that the point z is not too close to the free surface. Dimensional considerations now imply that

$$v' = (Q/Dd)F(Re, z/D) \tag{18}$$

where Q/Dd is a characteristic system velocity and

$$Re = (Q/Dd)(D/\nu) \tag{19}$$

is a system Reynolds number. At sufficiently high Re the dependence on Re in equation (18) should disappear, consistent with equation (17) which is based on the high Reynolds number turbulence model.

Figures 2 and 3 show data taken in the large system on the dependence of the r.m.s. values of the turbulent velocity components v_z' (vertical) and v_y' (horizontal) on Q/Dd and on z/D; the free surface elevation

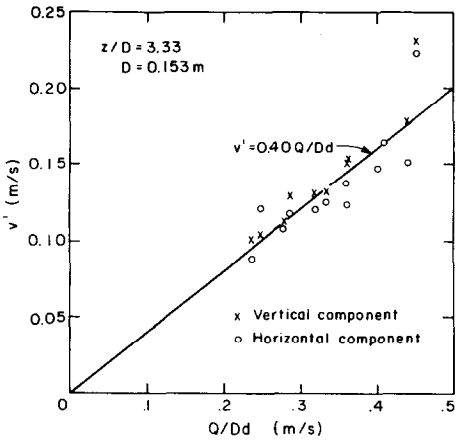

FIG. 2. Dependence of r.m.s. velocity components on Q/Dd.

was kept significantly above z. These data imply: (i) at $z/D > 3$ the turbulence is approximately isotropic in a horizontal plane; and (ii) the correlation for the r.m.s. value of either the horizontal or the vertical velocity component is

$$v' = 21.8(Q/Dd)\exp(-1.2z/D) \quad 3.1 < z/D < 4.2. \tag{20}$$

This Reynolds-number-independent correlation is consistent with the K–ε solution and implies that $\beta = 1.1$. The length scale which appears in the K–ε model is therefore

$$L = 1.1D. \tag{21}$$

Note that the length scale L is larger—by a factor of six in a constant-shear layer, where the relationship is known—than the 'mixing length', or characteristic eddy size, and the system Reynolds number Re is therefore correspondingly larger than a Reynolds number based on v' and a mixing length or eddy size.

The calibration of the small system showed that a Reynolds number dependence set in at $Re < 25 \times 10^3$. This point is illustrated in Fig. 4, which shows that at a fixed z/D of 3.3, the function F in equation (18)

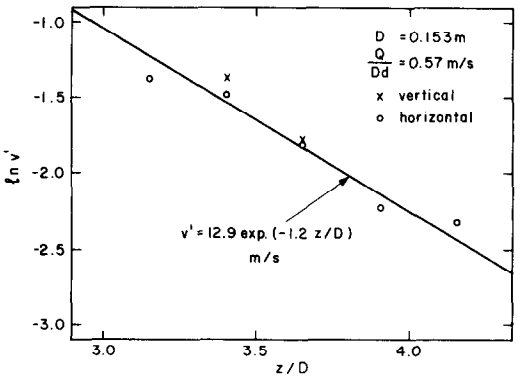

FIG. 3. Dependence of r.m.s. velocity components on z/D.

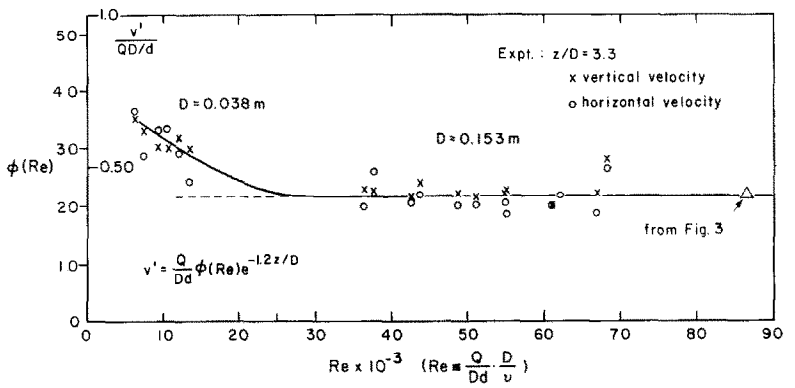

FIG. 4. The function $\phi(Re)$ in the correlation for v'.

begins to increase above its high Reynolds number value as Re is reduced below the critical value. The dependence on z/D, however, appears to be independent of Re down to the lowest values of our experiment. This is implied by the heat transfer data (see below). Hence, the data as a whole suggest a correlation of the form

$$v' = (Q/Dd)\phi(Re)\exp(-1.2z/D) \quad 3.1 < z/D < 4.2 \tag{22}$$

where

$$\begin{aligned} \phi(Re) &= 21.8 && Re > 25\times 10^3 \\ &= \text{as in Fig. 4} && Re < 25\times 10^3. \end{aligned} \tag{23}$$

The velocity samples were also analyzed for mean values to check the assumption that turbulent velocities dominated in the region of interest. The mean velocities showed considerable scatter. The average of the mean horizontal velocity components in the various samples was 0.7 cm s^{-1}, and the standard deviation 1.8 cm s^{-1}. This is to be compared with a typical r.m.s. velocity of 10 cm s^{-1}. The average of the vertical mean velocity determinations was 5.0 cm s^{-1}, and the standard deviation 1.8 cm s^{-1}. This was close to the independently measured, buoyant rise velocity of the particles, 5.6 cm s^{-1}. Hence, the assumption of small bulk flow appears to be borne out, at least approximately, in the region of interest.

Influence of free surface on turbulence. Figure 5 shows some measurements of v' at a fixed z while the free surface elevation above z was varied. The changes in the vertical and horizontal turbulent velocity as $(z_s-z)/D$ is reduced from 0.33 to 0.12 are within typical experimental scatter, although they do suggest the expected drop in the vertical turbulent velocity and rise in the horizontal turbulent velocity [31] as the surface is approached to within about $0.1D$–$0.2D$. We offer two conclusions. First, below about $0.3D$ of the surface the turbulence is essentially unaffected by the proximity of the surface. Secondly, and more tentatively, we estimate the damped layer thickness as being of order $0.1D$–$0.2D$. Based on the K–ε length scale

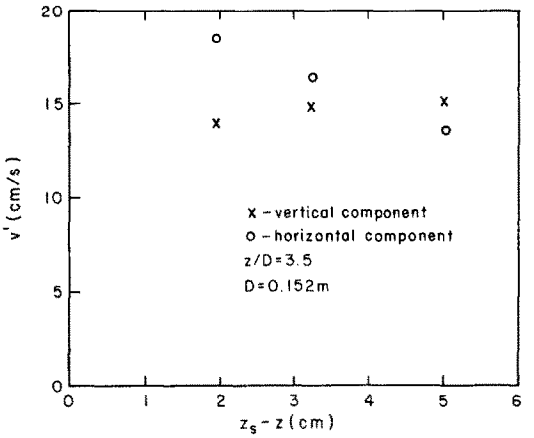

FIG. 5. Turbulent r.m.s. velocity components vs depth z_s-z below surface.

determined before, this is also the order of magnitude of the mixing length in this system.

4.2. *Condensation heat transport coefficient*

Data correlation in terms of system and turbulence parameters. Figures 6 and 7 show data for the con-

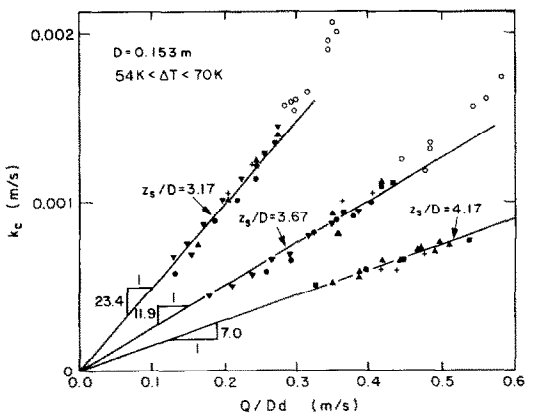

FIG. 6. Condensation coefficient as a function of the system parameters Q/Dd and z_s/D. The open circles denote data points rejected because of excessive surface waviness.

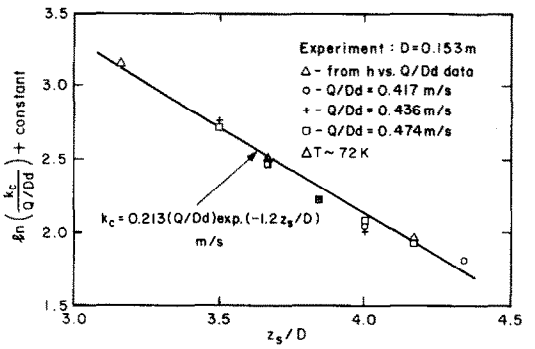

FIG. 7. Condensation coefficient as a function of surface elevation z_s/D.

densation coefficient k_c in the large system as a function of the system parameters Q/Dd and z_s/D, z_s being the elevation of the surface above the nozzle exit. The coefficient is defined in equation (9), and obtained from equation (11). As discussed earlier, the range of the data was limited by the need to have the turbulence intensity high enough to prevent damping of the turbulence by stable stratification on the one hand, and not so high that surface waves would significantly increase interfacial area above $\pi D^2/4$ on the other. Some of the points which were rejected because of surface waves are shown in Fig. 6 as open circles.

All the condensation data from the large system can be correlated in terms of system parameters with the equation

$$k_c = 0.213(Q/Dd)\exp(-1.2z_s/D). \quad (24)$$

A comparison with equation (20) yields the following relation between k_c and the turbulence parameters:

$$k_c = 0.0098v_s'. \quad (25)$$

Here, v_s' is obtained by extrapolating $v'(y)$ from the undamped region to the free surface elevation (Fig. 8). Equation (25) appears to correlate the data at all subcooling values.

In the small system, where the turbulence length

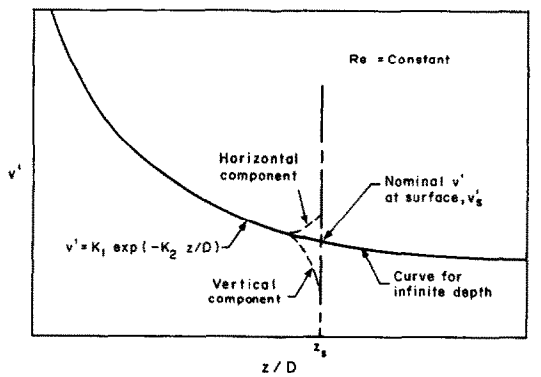

FIG. 8. Definition of v_s', the value of v' extrapolated from the bulk of the liquid to the surface.

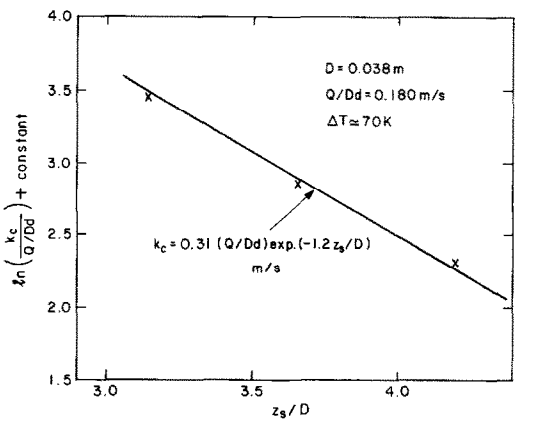

FIG. 9. Condensation coefficient as a function of z_s/D in the small system.

scale and Reynolds numbers are lower by a factor of four, the exponential fall-off of k_c with z_s/D is essentially the same as in the large system (Fig. 9), but the values of k_c at the same z_s/D and Q/Dd are larger. However, when the data are plotted against the turbulence parameters using equations (22) and (23), the small system data also satisfy the correlation expressed by equation (25). Figure 10 shows all data from both systems and at all values of subcooling as a correlation against v_s'.

Although the velocity dependence of equation (25) is consistent with the viscous inner-layer model of Table 1, it should be noted that it implies and *independence* of the Prandtl number based on *bulk* water temperature. This is further illustrated in Fig. 11, which shows the condensation rate at fixed turbulence and surface conditions over a range of water temperature. The bulk water viscosity and the bulk Prandtl number decrease by a factor of two as the subcooling decreases from 70 to 30 K. No significant change occurs in k_c.

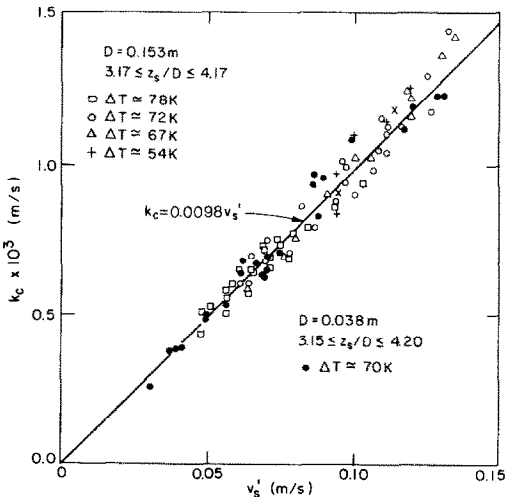

FIG. 10. Correlation for the condensation coefficient of atmospheric steam onto turbulent water.

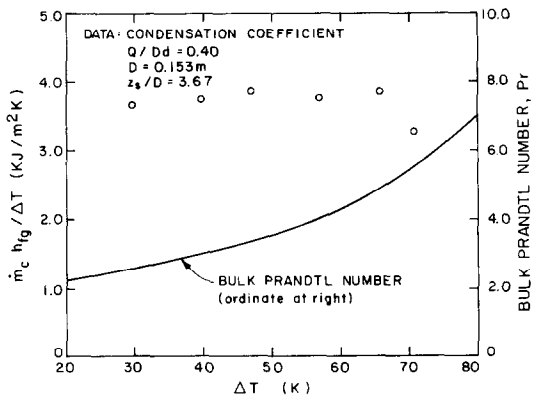

FIG. 11. Effect of water subcooling on condensation coefficient.

General correlation. The data presented here are for the condensation of atmospheric steam onto subcooled water. One can, however, draw from them some more general conclusions about the condensation coefficient for a vapor onto a turbulent liquid. We proceed in the simplest possible terms. Assume first of all that the general form of k_c will depend on the liquid-side turbulence, which we characterize by v_s' and the macroscale Λ. Secondly, it will depend on the liquid properties. We assume that the density, specific heat and thermal conductivity are essentially constant throughout the liquid (in water these quantities vary by about 4%, 0% and 12%, respectively, as the temperature rises from 25 to 100°C) and characterize them by their surface values ρ_s, c_{ps} and λ_s. The choice of surface vs bulk quantities is arbitrary, but motivated by the recognition that the thermal conductivity, which varies most, affects the condensation rate most critically very near the free surface. The viscosity, however, depends strongly on temperature (in water it decreases by a factor of three as the temperature rises from 25 to 100°C), and the form of this dependence may affect k_c. The viscosity coefficient of any liquid can be expressed approximately as [32]

$$\mu = \mu_s \exp\left[3.8(T_s/T - 1)\right] \tag{26}$$

where T_s is the saturation temperature and μ_s is the value of the viscosity at that temperature. Hence, the viscosity is characterized by two parameters, T_s and μ_s, in addition to the local temperature. Finally, the condensation coefficient is also affected by the latent heat of condensation, which controls the relative magnitudes of the conductive and convective heat fluxes at the surface (see Section 2.2). In summary, the condensation coefficient has the dependence

$$k_c = k_c(v_s', \Lambda, \rho_s, \lambda_s, c_{ps}, \mu_s, T_s, \Delta T, h_{fg}) \tag{27}$$

which implies that the general correlation must have the form

$$k_c/v_s' = f(\rho_s v_s' \Lambda/\mu_s, Pr_s, \Delta T/T_s, c_{ps}\Delta T/h_{fg}) \tag{28}$$

where we have dropped a fifth dimensionless independent variable, $c_{ps}\Delta T/v'^2$ because heating due to (turbulent) viscous dissipation has a negligible effect on the condensation coefficient in this problem. In equation (28)

$$Pr_s \equiv c_{ps}\mu_s/\lambda_s \tag{29}$$

is the liquid Prandtl number, evaluated at saturation (i.e. surface) conditions.

The last parameter in equation (28), $c_{ps}\Delta T/h_{fg}$, measures the effect of condensation mass flow on k_c [see equations (8) and (10)]. One can straightforwardly show that this parameter is essentially equal to the Péclet number based on the bulk condensation flow speed $u = \dot{m}_c/\rho$ normal to the surface, the thermal diffusion layer thickness $\delta = \rho c_{ps}\Delta T/\dot{m}_c h_{fg}$, and the thermal diffusivity α. For steam and water this parameter is small, and its effect on k_c should be small. Hence, if there is a dependence on the temperature difference between bulk and surface conditions, it will appear as a dependence on the parameter $\Delta T/T_s$, and will occur because the viscosity depends strongly on temperature.

Figure 12 shows all our data for k_c/v_s', plotted against the Reynolds number based on saturation conditions,

$$Re_s = \frac{\rho_s v_s' D}{\mu_s} \tag{30}$$

which in our system is proportional to the Reynolds number $\rho_s v' \Lambda/\mu_s$ which appears in equation (28). If Λ is identified with the length scale L in the K–ε model, the latter is $1.1Re_s$ [see equation (21)]. L is, however, usually significantly larger than a more conventionally defined macroscale.

Figure 12 implies that in the range of parameters investigated, k_c/v_s' has a constant value of 0.0098 independent of Re_s, $\Delta T/T_s$ and $c_{ps}\Delta T/h_{fg}$. Bulk water temperatures from 22 to 70°C are included, so that $\Delta T/T_s$ varies from 0.08 to 0.21 and $c_{ps}\Delta T/h_{fg}$ from 0.05 to 0.13. The lack of dependence on $\Delta T/T_s$ is emphasized in Fig. 11. The dependence on Pr_s is not established by these data, the value of Pr_s being fixed at 1.76.

Assuming that the dependence on Pr_s is separable from those of the other parameters in equation (28), we can conclude that, for a shear-free surface with horizontally isotropic turbulence imposed from below, the condensation coefficient has the general form

$$\begin{aligned} k_c/v_s' &= f(Pr_s) \\ &= 0.0098 \quad \text{for} \quad Pr_s = 1.76 \\ 4 \times 10^3 &< Re_s < 72 \times 10^3 \\ \Delta T/T_s &< 0.21 \\ c_{ps}\Delta T/h_{fg} &< 0.13. \end{aligned} \tag{31}$$

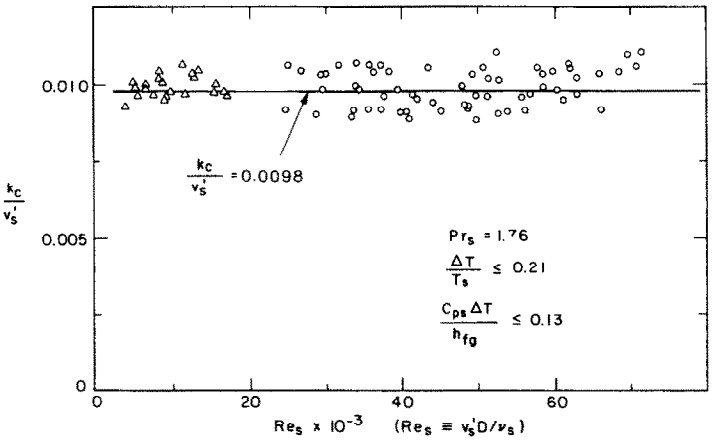

FIG. 12. Data correlation for condensation at $Pr_s = 1.76$.

Here v_s' is the r.m.s. value of either the vertical or horizontal component of turbulent velocity, extrapolated to the surface from the bulk of the liquid to the damped layer (Fig. 8). The lower limits of the two temperature parameters have been set to zero because these parameters will have a progressively smaller effect on k_c as their values decrease.

The implication of equation (31) is that k_c/v_s' depends only on the molecular transport properties evaluated at surface conditions, although the form of this dependence has not been established in the present study.

5. DISCUSSION OF STEADY-STATE DATA

Surprisingly, the only two conceptual models in Table 1 which have a velocity dependence similar to our data are the viscous inner-layer model and Kishinevsky's model, neither of which was intended for conditions similar to our experiments. Kishinevsky's model presumes a rough, highly agitated surface; our data are for a calm and essentially smooth surface. The inner-layer model assumes that the liquid-side turbulence is generated by a mean shear stress at the interface, in which case the turbulence macroscale is a dependent variable and does not enter the correlation for k_c; in our experiments the turbulence was generated by external means below the surface, and there is no *a priori* reason to assume that k_c should be independent of the macroscale.

Another interesting attribute of our correlation is its apparent lack of dependence on the bulk liquid properties, and its implication that only the properties at surface conditions can affect the transport significantly. This implies that the liquid properties affect the transport rate on a scale which is much smaller than the thermal layer thickness δ across which the mean temperature and other liquid properties change from their surface to their bulk values. Using the estimate

$$\delta \equiv \alpha_s/k_c \qquad (32)$$

with k_c taken from equation (31), one obtains for our experiments, with $v_s' \simeq 0.1$ m s^{-1}, $\delta \simeq 0.17$ mm. The turbulence macroscale Λ in the bulk was almost two orders of magnitude larger than this value. The only length scale which was comparable with δ or smaller in our tests was the Kolmogorov microscale. The implication is that the transport rate across the interface is controlled by processes at the level of the turbulence microscale. In Table 1, only the viscous inner-layer model has both this attribute and a velocity dependence which agrees with our correlation.

The time scale τ of the surface-renewing eddies is obtained by equating equations (10) and (31). For our case of atmospheric steam condensing on subcooled water, one obtains $\tau = 7.1 \times 10^{-4}/v_s'^2$. Note that this can also be written $\tau = 2.4 \times 10^3 \nu_s/v_s'^2$, which would suggest that to the extent that the inner-layer model (with viscosity based on surface conditions and u^* replaced by v_s') has any credence, the eddies responsible for the mass transport across the interface have relatively long time scales compared with the typical eddies in the inner layer. While parallels are premature, this result is at least not inconsistent with Campbell and Hanratty's study [33] of mass transport at a solid boundary, where they found the median period $2\pi/\omega$ of the mass transfer fluctuations to be of order $10^3 \nu/v'^2$.

Comparison with other condensation data

To the authors' knowledge, the only other data available for steam condensation at a shear-free, turbulent interface are those of Thomas [34]. Thomas investigated condensation in several different systems, including a vertical-jet system which was superficially similar to ours, but actually quite different in that his test cell was relatively shallow, with z_s/D in the range 0.3–1.3. As a result, his system produced not a bulk-flow-free turbulence like ours, but a radial bulk outflow in a thin, turbulent boundary layer under the surface, with the mean velocity at the surface falling

off inversely with r. Thomas obtained an empirical correlation for the mean velocity at the surface as a function of radial position, but did not report turbulence intensities. This rules out a direct comparison with our present correlation. However, if one assumes that the local r.m.s. turbulent velocity v' is some fraction γ of the mean velocity at the surface, and integrates our correlation equation [equation (31), with $Pr_s = 1.76$] over the surface of Thomas's system using his correlation (see his Fig. 6a) for the mean velocity at the surface as a function of r, one obtains a result which is in good agreement with that body of Thomas's data for which the surface was not broken up, provided γ is taken to be about 0.1—a reasonable value. Reasonable agreement is also obtained with Thomas's data for his other systems if one predicts the condensation heat transfer by integrating our equation (31) over the system surface with his rough estimates (Thomas's Table 1) of local turbulence intensity for v_s'. The predictions based on our correlation show a linear dependence on Reynolds number, in agreement with Thomas's data, rather than the 3/4 or 1/2 power Thomas was looking for based on the model proposed by Theofanous *et al.* [13].

Jensen and Yuen [9] measured both steam condensation rates and turbulence intensities in open-channel flows where the liquid-side turbulence was induced mainly by the shear stress exerted by the flowing steam. When the steam shear controlled the condensation rate, the surface had a 'pebbled', wavy appearance, and Jensen and Yuen found k_c to be proportional to the shear velocity. They suggested a data correlation $k_c = 0.14 Pr_w^{-1/2} u_s^*$, where u_s^* is the shear velocity based on the interfacial shear stress and liquid density and Pr_w is the molecular Prandtl number based on bulk liquid properties. The Prandtl number dependence was postulated, Pr_w having been fixed at a value 6.2 in all their experiments. Based on LDA measurements, Jensen and Yuen found the r.m.s. value u_s' of the turbulent velocity component in the flow direction to be $u_s' \simeq 2.9 u_s^*$. Hence, their proposed correlation corresponds to

$$k_c \simeq 0.019 u_s' \quad (Pr_s = 1.76). \tag{33}$$

The coefficient in this correlation is about twice the value of that in equation (32), and would be even larger if the average of the r.m.s. velocity components were used instead of u'. This suggests that the condensation coefficient is not controlled just by the value of v_s' at the interface, but depends also on how the turbulence is generated, i.e. on the structure of the turbulence field.

Comparison with gas absorption data

Our data do not provide information on the dependence of k_c on the Prandtl number Pr_s, nor are we aware of suitable condensation data at values of Pr_s significantly different from 1.76. Some idea of the Prandtl number dependence can, however, be obtained by comparing our data with that for gas absorption into water, where the Schmidt number is very high. $k_c(Pr_s, v_s')$ and $k(Sc, v_s')$ should have similar functional forms.

Gas absorption rates have been measured in turbulent channel flows without shear at the interface by Krenkel and Orlob [16] and Eloubaidy [see 18]. Krenkel and Orlob's correlation for the transport of oxygen into water at a nominal 20°C can be written $k = 1.37 \times 10^{-4} D_L/H$, where k is defined by equation (1), H is the water depth and D_L is the effective streamwise dispersion coefficient (the Taylor dispersion coefficient) in the channel flow. For open-channel flow Elder [35] obtained the experimental relation $D_L = 6.3 u^* H$, where u^* is the shear velocity on the channel floor. Hence, Krenkel and Orlob's correlation can be written $k = 8.65 \times 10^{-4} u^*$. Eloubaidy's data, as quoted by Plate and Friedrich [18], imply a similar correlation with a coefficient 9.83×10^{-4}. According to Plate and Friedrich, the r.m.s. value of the streamwise fluctuating velocity component u_s' at the surface is approximately equal to u^* (Komori *et al.* [31] put it somewhat lower, however). Hence we have, approximately, for turbulent channel flow without interfacial shear

$$k \simeq 0.9 \times 10^{-3} u_s' \quad (Sc = 500,\ 800 < u_s' H/\nu < 7400) \tag{34}$$

where the quoted Reynolds number range spans the two sets of data.

Figure 13 shows both equation (34) and our own equation (31) as data points on a plot of k/u_s' vs Sc or k_c/v_s' vs Pr_s. These two points are hardly sufficient to imply a functional relationship; indeed, they are not even strictly comparable since the turbulence in the channel flow is not horizontally isotropic, and u_s' and v_s' are not identical quantities. About all we can conclude is that the relations

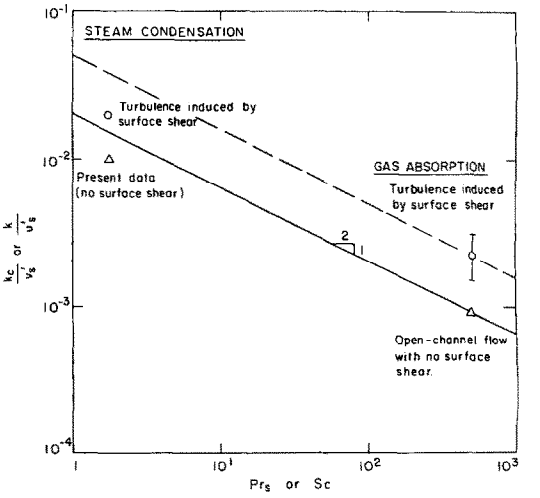

FIG. 13. Transport coefficients for steam condensation and gas absorption on water.

$k/u_s' \sim Sc^{-1/2}$ or $k_c/v_s' \sim Pr_s^{-1/2}$ at high Schmidt or Prandtl numbers (e.g. [22]) are not ruled out.

Gas absorption data are also available for channel flows with wind-induced shear. For these, Aisa *et al.* [14] and McCready and Hanratty [15] have proposed correlations of the form $k = (0.1\text{–}0.2)Sc^{-1/2}u_s^*$, where u_s^* is the shear velocity based on interfacial shear and liquid density. This correlation agrees with other data (e.g. [36, 10]) for similar flow conditions. If we accept Jensen and Yuen's result (obtained, one should note, in the presence of condensation) that $u_s' \simeq 2.9u^*$, the correlation implies that at a nominal Schmidt number of 500 which is typical of the gas absorption experiments

$$k \simeq (1.5\text{–}3.1)\times 10^{-3}u_s' \quad (Sc \simeq 500,\ u_s'H/\nu > 120). \tag{35}$$

The lower Reynolds number limit is prescribed by McCready and Hanratty's data, which indicate that at Reynolds numbers below 120, the transport coefficient drops off rapidly. Comparing equations (35) and (34), and (33) and (31), it appears that at similar turbulence intensities at the interface, the transport rate is roughly a factor of two higher when the turbulence is induced by surface shear than when it is generated from below the surface. Both data sets show k being proportional to v' and, given the uncertainties in the comparisons, at least do not rule out k/v' being proportional to $Pr^{-1/2}$ or $Sc^{-1/2}$ at high Pr or Sc (Fig. 13).

6. CONCLUSIONS

Equation (31) expresses the rate correlation for steady condensation of vapor onto a shear-free and relatively wave-free liquid interface in which the turbulence is produced from below and is essentially isotropic in the horizontal plane. The condensation rate is proportional to the r.m.s. turbulence velocity at the surface, and independent of the turbulence macroscale. The proportionality coefficient appears to depend only on the Prandtl number Pr_s of the liquid at the surface (i.e. at saturation conditions); the present study establishes its value only for $Pr_s = 1.76$, corresponding to atmospheric steam condensing on subcooled water.

REFERENCES

1. J.-H. Chun, M. A. Shimko and A. A. Sonin, Vapor condensation onto a turbulent liquid—II. Condensation burst instability at high turbulence intensities, *Int. J. Heat Mass Transfer* **29,** 1333–1338 (1986).
2. T. G. Theofanous, Conceptual models of gas exchange. In *Gas Transfer at Water Surfaces* (Edited by W. Brutsaert and G. H. Jirka), pp. 271–281. Reidel, Dordrecht (1984).
3. R. Higbie, The rate of absorption of a pure gas into a still liquid during short periods of exposure, *Trans. A.I.Ch.E.* **31,** 365–389 (1935).
4. V. G. Levich, *Physicochemical Hydrodynamics.* Prentice-Hall, Englewood Cliffs, NJ (1962).
5. C. J. King, Turbulent liquid phase mass transfer at a free gas–liquid interface, *Ind. Engng Chem. Fundam.* **5,** 1–8 (1966).
6. H. Ueda, R. Moller, S. Komori and T. Mizushina, Eddy diffusivity near the free surface of open channel flow, *Int. J. Heat Mass Transfer* **20,** 1127–1136 (1977).
7. G. E. Fortescue and J. R. A. Pearson, On gas absorption into a turbulent liquid, *Chem. Engng Sci.* **22,** 1163–1176 (1967).
8. J. C. Lamont and D. S. Scott, An eddy cell model of mass transfer into the surface of a turbulent liquid, *A.I.Ch.E. Jl* **16,** 513–519 (1970).
9. R. J. Jensen and M. C. Yuen, Interphase transport in horizontal stratified concurrent flow, U.S. Nuclear Regulatory Commission Report NUREG/CR-2334 (1982).
10. M. Sivakumar, Reaeration and wind induced turbulence shear in a contained water body. In *Gas Transfer at Water Surfaces* (Edited by W. Brutsaert and G. H. Jirka), pp. 369–377. Reidel, Dordrecht (1984).
11. W. H. Henstock and T. J. Hanratty, Gas absorption by a liquid layer flowing on the wall of a pipe, *A.I.Ch.E. Jl* **25,** 122–131 (1979).
12. M. Kh. Kishinevsky, Two approaches to the theoretical analysis of absorption processes, *J. appl. Chem. USSR* **28,** 881–886 (1955) (translation pagination).
13. T. G. Theofanous, R. N. Houze and L. K. Brumfield, Turbulent mass transfer at free, gas–liquid interfaces, with application to open-channel, bubble and jet flows, *Int. J. Heat Mass Transfer* **19,** 613–624 (1976).
14. A. Aisa, B. Caussade, J. George and L. Masbernat, Echangez de gaz dissous en ecoulements stratifies de gaz et de liquide, *Int. J. Heat Mass Transfer* **24,** 1008–1018 (1981).
15. M. J. McCready and T. J. Hanratty, A comparison of turbulent mass transfer at gas-liquid and solid-liquid interfaces. In *Gas Transfer at Water Surfaces* (Edited by W. Brutsaert and G. H. Jirka), pp. 283–292. Reidel, Dordrecht (1984).
16. P. A. Krenkel and G. T. Orlob, Turbulent diffusion and the reaeration coefficient, *J. Sanitary Engng Div., Proc. ASCE* **88**(SA2), 53–82 (1962).
17. A. F. Eloubaidy, E. J. Plate and J. Gessler, Wind waves and the reaeration coefficient in open channel flow, Report No. CER 69.70 AFE 2, Department of Civil Engineering, Colorado State University (1969).
18. E. J. Plate and R. Friedrich, Reaeration of open channel flow. In *Gas Transfer at Water Surfaces* (Edited by W. Brutsaert and G. H. Jirka), pp. 333–346. Reidel, Dordrecht (1984).
19. Y. S. Won and A. F. Mills, Correlation of the effects of viscosity and surface tension on gas absorption rates into freely falling turbulent liquid films, *Int. J. Heat Mass Transfer* **25,** 223–229 (1982).
20. A. K. Bin, Mass transfer into a turbulent liquid film, *Int. J. Heat Mass Transfer* **26,** 981–991 (1983).
21. M. Kh. Kishinevsky and V. T. Serebryansky, The mechanism of mass transfer at the gas–liquid interface with vigorous stirring, *J. appl. Chem. USSR* **29,** 29–33 (1956) (translation pagination).
22. J. J. Ledwell, The variation of the gas transfer coefficient with molecular diffusivity. In *Gas Transfer at Water Surfaces* (Edited by W. Brutsaert and G. H. Jirka), pp. 293–302. Reidel, Dordrecht (1984).
23. J. T. Davies, A. A. Kilner and G. A. Ratcliff, The effect of diffusivities and surface films on rates of gas absorption, *Chem. Engng Sci.* **19,** 583–590 (1964).
24. M. Barchilon and R. Curtet, Some details of the structure of an axisymmetric confined jet with backflow, *ASME J. Basic Engng* 777–787 (1964).
25. E. J. Hopfinger and J. A. Toly, Spatially decaying tur-

bulence and its relation to mixing across density interfaces, *J. Fluid Mech.* **78,** 155–175 (1976).
26. S. M. Thompson and J. S. Turner, Mixing across an interface due to turbulence generated by an oscillating grid, *J. Fluid Mech.* **67,** 349–368 (1975).
27. B. Brumley, Turbulence measurements near the free surface in stirred grid experiments. In *Gas Transfer at Water Surfaces* (Edited by W. Brutsaert and G. H. Jirka), pp. 83–92. Reidel, Dordrecht (1984).
28. M. A. Shimko, Scalar Transport at a Turbulent Liquid Free Surface. M.S. thesis, Department of Mechanical Engineering, MIT (1985).
29. W. P. Jones and B. E. Launder, The prediction of laminarization with a two-equation model of turbulence, *Int. J. Heat Mass Transfer* **15,** 301–313 (1972).
30. S. B. Pope and J. H. Whitelaw, The calculation of near-wake flows, *J. Fluid Mech.* **73,** 9–32 (1976).
31. S. Komori, H. Ueda, F. Ogino and T. Mizushina, Turbulence structure and transport mechanism at the free surface in open channel flow, *Int. J. Heat Mass Transfer* **25,** 513–521 (1982).
32. J. O. Hirschfelder, C. F. Curtiss and R. Bird, *Molecular Theory of Gases and Liquids.* Wiley, New York (1964).
33. J. A. Campbell and T. J. Hanratty, Turbulent velocity fluctuations that control mass transfer to a solid boundary, *A.I.Ch.E. Jl* **29,** 215–221 (1983).
34. R. M. Thomas, Condensation of steam on water in turbulent motion, *Int. J. Multiphase Flow* **5,** 1–15 (1979).
35. J. W. Elder, The dispersion of marked fluid in turbulent shear flow, *J. Fluid Mech.* **5,** 544–560 (1959).
36. J. Tsacoyannis, These du Grade de Docteur-Ingenieur, L'Universite Paul-Sabatier de Toulouse (1969).

CONDENSATION DE VAPEUR SUR UN LIQUIDE TURBULENT—I. CONDENSATION PERMANENTE FONCTION DE LA TURBULENCE DU COTE DU LIQUIDE

Résumé—On présente des résultats expérimentaux sur la condensation de vapeur sur un liquide turbulent, la turbulence étant isotrope dans le plan horizontal et l'interface sans cisaillement et relativement sans ondes. Une formule est proposée pour le coefficient de condensation en fonction de l'intensité de la turbulence du coté du liquide, la micro-échelle de turbulence et le sous-refroidissement.

KONDENSATION AN EINER TURBULENTEN FLÜSSIGKEIT— I. DIE STATIONÄRE KONDENSATIONSRATE ALS FUNKTION DER TURBULENZ DER FLÜSSIGKEIT

Zusammenfassung—Es werden Ergebnisse über die Kondensation von Dampf an einer turbulenten Flüssigkeit mitgeteilt, wobei die Turbulenz in der horizontalen Ebene isotrop ist, die Kernströmung frei ist und die Grenzfläche ohne Schubspannung und verhältnismäßig frei von Wellen ist. Für den Übergangskoeffizienten wird in Abhängigkeit von der Turbulenzintensität der Flüssigkeit, vom Turbulenzmaßstab und von der Unterkühlung eine Korrelation vorgeschlagen.

КОНДЕНСАЦИЯ ПАРА НА ТУРБУЛЕНТНОМ ПОТОКЕ ЖИДКОСТИ—I. УСТАНОВИВШАЯСЯ СКОРОСТЬ КОНДЕНСАЦИИ КАК ФУНКЦИЯ ТУРБУЛЕНТНОСТИ ПРИГРАНИЧНОЙ ЖИДКОСТИ

Аннотация—Приведены данные по скорости и конденсации пара на турбулентном потоке, причем считается, что турбулентность изотропна в горизонтальной плоскости, а на межфазной поверхности отсутствуют сдвиги и волны. Для коэффициента скорости конденсации предложено выражение через интенсивность турбулентности жидкости, макромасштаб турбулентности и недогрев.